The gliopeptide ODN, a ligand for the benzodiazepine site of $GABA_A$ receptors, boosts functional recovery after stroke

Rhita Lamtahri[1], Mahmoud Hazime[1], Emma K Gowing[2], Raghavendra Y. Nagaraja[2], Julie Maucotel[3], Pascale Quilichini[4], Katia Lehongre[5], Benjamin Lefranc[1,6], Katarzyna Gach-Janczak[1,7], Ann-Britt Marcher[8], Susanne Mandrup[8], David Vaudry[1,6], Andrew N. Clarkson[2,*], Jérôme Leprince[1,6,*] and Julien Chuquet[1,*]

[1] Normandie Univ, UNIROUEN, INSERM U1239, Neuronal and Neuroendocrine Differentiation and Communication, Rouen, France.
[2] Department of Anatomy, Brain Health Research Centre and Brain Research New Zealand, University of Otago, Dunedin 9054, New Zealand.
[3] Normandie Univ., UNIROUEN, Animal Facility, Rouen, France.
[4] Neurosciences Systems Institute, INSERM UMR-S 1106, Aix Marseille University, Marseille, France.
[5] ICM Brain and Spine Institute, Paris, France.
[6] Normandie Univ, PRIMACEN, Institute for Research and Innovation in Biomedicine, Rouen, France.
[7] Department of Biomolecular Chemistry, Medicinal University of Łódź, Łódź, Poland.
[8] Department of Biochemistry and Molecular Biology, University of Southern Denmark, Odense, Denmark.

Corresponding author: Julien Chuquet, University of Rouen Normandie, INSERM U1239, 76821, Mont-Saint-Aignan, France. Tel.: +33 235 146 047. Email: julien.chuquet@univ-rouen.fr

* ANC, JL and JC contributed equally to this work.

The authors have declared that no conflict of interest exists.

Abstract

Following stroke, the survival of neurons and their ability to re-establish connections is critical to functional recovery. This is strongly influenced by the balance between neuronal excitation and inhibition. In the acute phase of experimental stroke, lethal hyperexcitability can be attenuated by positive allosteric modulation of $GABA_A$ receptors ($GABA_AR$). Conversely, in the late phase, negative allosteric modulation of $GABA_AR$ can correct the sub-optimal excitability and improves both sensory and motor recovery. Here, we hypothesized that octadecaneuropeptide (ODN), an endogenous allosteric modulator of the $GABA_AR$ synthesized by astrocytes, influences the outcome of ischemic brain tissue and subsequent functional recovery. We show that ODN boosts the excitability of cortical neurons, which make it deleterious in the acute phase of stroke. However, if delivered after day 3, ODN is safe and improves motor recovery over the following month in both young and aged mice. Furthermore, we bring evidence that during the sub-acute period after stroke, the repairing cortex can be treated with ODN by means of a single hydrogel deposit into the stroke cavity.

Introduction

Stroke remains a devastating clinical challenge because there is no efficient therapy to either minimize neuronal death with neuroprotective drugs or to enhance spontaneous recovery with neurorepair drugs. The chronic and ever-changing balance between neuronal excitation and inhibition is a primary trigger for the initial stroke progression as well as the impairment in the ability to regain function. Given its predominant role in the control of inhibition, GABAergic transmission remains a major target to act on the dynamic of this balance (Bachtiar and Stagg, 2014; Roux and Buzsáki, 2015). The use of pharmacological manipulations targeting $GABA_A$ receptors ($GABA_AR$) to modify the course of ischemic cell damage and their sequelae is an old quest: numerous pre-clinical experiments have demonstrated that sustaining GABA neurotransmission, to counteract the initial excitotoxic effect of glutamate released minutes to hours after the onset of stroke can afford protection (Sydserff *et al*., 1995; Shuaib and Kanthan, 1997, Green *et al.,* 2000; Schwartz-Bloom and Sah, 2001; Marshall *et al*., 2003). In this respect, benzodiazepines with positive allosteric modulation (PAM) profile were repeatedly shown to be neuroprotective after cerebral ischemia (Schwartz *et al.,* 1994 and 1995; Schwartz-Bloom *et al.,* 1998; Galeffi *et al.,* 2000). However, like all neuroprotective drug therapies to-date, positive GABA modulators have failed to translate into clinical use.

In recent years, GABA modulation in stroke has been revitalized with the understanding that once the infarction is consolidated, the excitation and inhibition balance switches from hyperexcitability to hypoexcitability in the peri-infarct cortex, due to a loss of the astroglial GABA tranporter, GAT3, and resultant excess in ambient GABA (Clarkson *et al.,* 2010; Carmichael, 2012). This prolonged synaptic

depression is thought to limit neuronal circuit reorganization and therefore the regain of sensorimotor functions (Kim *et al.,* 2014; Hummel et al., 2009). Dampening the stroke-induced elevation in inhibition using a negative allosteric modulator (NAM) targeting the benzodiazepine site of $GABA_AR$, enhances sensorimotor recovery in mice and rats (Clarkson *et al.,* 2010, 2015; Lake *et al.,* 2015; Alia et al., 2016; Orfila et al., 2019).

Endozepines, known as the endogenous ligands of benzodiazepine-binding sites, comprise the diazepam binding inhibitor (DBI, also known as acyl-CoA binding protein, ACBP) and its processing products, including the octadecaneuropeptide (ODN), a small peptide of 18 amino-acids (DBI_{33-50}) (Tonon et al., 2019). In the brain, DBI is one of the major proteins expressed and released by astrocytes but not by neurons (Loomis *et al.,* 2010; Tonon *et al.,* 2019). DBI and ODN bind to the benzodiazepine site of the $GABA_AR$ where they act as allosteric neuromodulators (Bormann, 1991; Barmack *et al.,* 2004; Quian *et al*., 2008; Möhler, 2014; Dumitru *et al.,* 2017). Point mutation targeting the benzodiazepine site of $GABA_AR$ renders neuronal cells insensitive to ODN (Dumitru et al., 2017). At micromolar concentrations, electrophysiological studies show that ODN acts as a NAM on $GABA_ARs$, i.e. reducing $GABA_AR$ mediated inhibition (Guidotti *et al.,* 1983; Ferrero *et al.,* 1986; Barmack *et al.,* 2004; Alfonso et al., 2012; Dumitru *et al.,* 2017) with no epileptogenic effect (Vezzani et al., 1991). ODN appears to be a relatively new astroglial modulator of $GABA_AR$ signaling and should therefore be considered for its potential to correct the imbalance between excitation and inhibition that arises as a consequence of a stroke. Here, we tested the gliopeptide ODN for its potency to enhance recovery after stroke. We show that ODN boosts the excitability of cortical neurons, which make it deleterious in the acute phase of stroke. However, if

delivered after day 3, ODN is safe and improves motor recovery in two different models of focal brain ischemia. Furthermore, we bring novel evidence that during the sub-acute period after stroke, the repairing cortex can be treated with ODN by the means of a single hydrogel injection into the stroke cavity allowing for direct targeting of the peri-infarct cortex.

Results

Effect of ODN on cortical activity

Changes in neuronal excitation is critical for cell survival during the acute phase of stroke as well as for synaptic plasticity and recovery during the repair phase after stroke. To address the general hypothesis that extrinsic ODN can be used to safely manipulate neuronal excitability and influence post-ischemic repair, we first checked whether, as reported previously *in vitro*, ODN induced a measurable enhancement of cortical activity. In isoflurane-anesthetized mice, we recorded the effect of 1 µg of ODN or its vehicle on neuronal spiking of layer 4 of the somato-sensory cortex (Figure 1A). Inspection of electrophysiological recordings did not reveal any aberrant oscillations or sharp events that would indicate epileptiform activity (Figure 1B). ODN increased spontaneous neuronal firing (181.5 ± 61.6% increase compared to the pre-treatment period; $P < 0.05$; n = 6 mice; vehicle: 4.7 ± 11.4%; $P > 0.05$; n = 6) while vehicle administration did not result in any significant change in spiking activity (Figure 1C). To further examine the potential of ODN to boost neuronal excitability, the effect of ODN was also tested during a somato-sensory stimulation. A single deflection of the whiskers pad triggered a somato-sensory evoked potential (SEP) in layer 4 of the contralateral barrel cortex (Figure 1, D and E). As a result of ODN treatment, SEP slopes increased by 147.8 ± 71.8% showing that ODN increases neuronal excitability ($P < 0.05$ vs. pre-treatment period; n = 6 mice; vehicle group: 4.7 ± 26.4%; $P > 0.05$ vs. pre-treatment period; n = 6; Figure 1, F and G). Furthermore, the positive effect of ODN on cortical activity was also revealed by the increase of astrocytic network activity seen by intravital calcium imaging using a two-photon microscope (Figure 1, H-J). Astrocytes displayed spontaneous calcium

transients at the frequency of 3.6 ± 1.4 mHz during the baseline period as previously described (Chuquet et al., 2007). After ODN administration, transient frequency rose to 7.5 ± 0.8 mHz ($P < 0.05$; n = 23 cells from 6 animals) whereas calcium activity was unaffected following vehicle administration (3.15 ± 0.7 mHz vs. 3.08 ± 0.8 mHz; $P > 0.05$; n = 16 cells from 5 animals; Figure 1, J and K). Overall these results show for the first time that the endozepine ODN acts as an excitability-enhancer of the cerebral cortex *in vivo*.

Acute effect of ODN during cerebral ischemia

Within the first minutes to hours after stroke onset, depolarization and hyperexcitability are the primary culprits for the massive necrotic neuronal loss. Although ODN has a potent neuroprotective effect *in vitro* (Hamdi et al., 2011), enhancing cortical excitability in the acute phase of brain ischemia, when excitation is already lethal for neurons, may be inimical to cell survival. In order to examine whether the subtle changes of cortical activity elicited by ODN could influence ischemic neuronal death processes, we administered ODN (1 µg intracerebroventricular, i.c.v) during the acute phase of a focal brain ischemia elicited by intraluminal occlusion of the right middle cerebral artery (MCAO). The transient ischemia (60 min followed by reperfusion) produced a reproducible infarct 48 h later (Figure 2A). Continuous laser Doppler flowmetry monitoring of the cerebral blood flow (CBF) confirmed that all animals underwent a similar ischemia and that ODN had no impact on residual CBF ($P > 0.05$ at any time point; Figure 2C). The treatment with ODN resulted in a severe aggravation of the mean infarction volume (51.7 ± 15.8% increase compared to the vehicle control group; $P < 0.05$; n = 8; Figure 2A). Physiological parameters well known to have a determinant impact on neuronal

survival in stroke (arterial pressure, temperature, food intake) were not affected by central administration of ODN (Figure 2, C-F). Flumazenil, a selective antagonist of the benzodiazepine-binding site of the $GABA_AR$, fully reversed ODN-induced exacerbation ($P > 0.05$; n = 8; Figure 2A) confirming the involvement of the GABAergic signaling. MCAO was also conducted on knockout mice for the DBI gene ($DBI^{-/-}$) and consistent with the above observations, $DBI^{-/-}$ animals appeared to be more resistant to MCAO than their wild-type counterparts (-40.1 ± 9.1%; $P < 0.05$; n = 6; Figure 2B). This result suggests that the endogenous production of the ODN precursor plays a role in the pathophysiology of stroke. In view of the above results, the most likely hypothesis for the ODN aggravated neuronal cell death, is due to a decrease in GABAergic inhibition, a well-documented pathway in neuroprotection and recovery (Green *et al.,* 2000; Clarkson *et al.,* 2010). This was further corroborated by two other observations. First, we examined the effect of ODN in the case of a pure excitotoxic neuronal cell death induced by a microinjection of NMDA. The co-administration of ODN with NMDA significantly increased the size of the excitotoxic lesion (3.5 ± 0.4 mm^3 vs. 6.4 ± 0.9 mm^3; $P < 0.05$; Figure 3, A and B). Second, another, albeit closely related pathophysiologic event, is spreading depressions (SD), *i.e.* waves of transient depolarization preceding cell damage in the compromised brain (Hartings *et al.,* 2017). Local application of KCl on the healthy cortical tissue triggers such SD events, as described elsewhere (Chuquet et al., 2007). We found that central administration of ODN 10 min before the induction of a train of 2-3 SDs, increased the number of events by 61.8% ($P < 0.05$ vs. vehicle group; n = 6; Figure 3, C and D). The amplitude and temporal features of SDs were unchanged by ODN ($P > 0.05$; n = 6; Figure 3E). In a condition of hyperexcitability like the one observed during the acute phase of ischemia, the neuroprotective

features of the gliopeptide ODN are surpassed by its pro-excitotoxic effect. Altogether, these observations are fully consistent with the view that the negative allosteric modulation of the $GABA_AR$ is not safe in the acute phase of stroke (Clarkson et al., 2010).

Effect of ODN on functional recovery after MCAO stroke

In the weeks following stroke, the peri-infarct surviving tissue is in a state of heightened neuronal plasticity, which is intended to promote the recovery of lost functions. Some of the repair processes that are altered rely on an increase in synaptic transmission and therefore depend on an optimal excitation/inhibition balance. Contrary to the acute phase of stroke (minutes, hours) where excitation must be decreased to maintain neuronal survival, in the chronic phase (weeks), an excess of GABAergic inhibition prevents optimal recovery (Clarkson *et al.,* 2010). Spurred by recent studies demonstrating that the exogenous benzodiazepine inverse agonist L655,708 is efficient in correcting this imbalance and improves the recovery of mice after stroke (Clarkson *et al.,* 2010; Lake *et al.,* 2015), we made a similar hypothesis that chronic treatment with the endozepine ODN would promote enhanced neuronal plasticity. To avoid any interactions of ODN with its effects on cell death during the acute phase of stroke, we began the treatment with the gliopeptide (or its vehicle) 72 h after the onset of stroke (Figure 4, A and B), a sufficient delay for the lesion to be fully formed and no further expansion observed beyond this period. Preoperative performances in the “latency to turn” task, the “latency to descend” task and the “latency to cross” task did not differ between the 4 different groups. Altogether these 3 behavioral tasks provided a well-established method for measuring weekly evolution of sensorimotor coordination and balance following

extended ischemic lesion (e.g. cortex and striatum) in rodents over a period of weeks following the initial insult (Matsuura *et al.,* 1997; Carter *et al.,* 2001). Unlesioned sham mice were not affected at any time-points, reporting that neither the surgery procedure, the ODN treatment, nor a learning effect interfered in the observations made from MCAO animals. Stroke induced a severe decrease in the ability to execute all three tasks (Figure 4, C-E), with only a small spontaneous gain of function observed over weeks 1 and 2 in the vehicle treated group. Treatment with ODN however, resulted in a marked improvement on all three task functions, with significance observed by weeks 3 and 4 post-stroke (Figure 4, C-E). Assessment on two of the three tasks revealed that the MCAO plus ODN treatment group was not significantly different when compared to unlesioned controls at day 28 post-stroke. ODN had no impact on stroke-induced weight loss, and mortality rate remained similar between ODN and vehicle-treated groups (Figure 4F). At 28 days post-stroke, brains were collected for further histological analysis. The lesion characteristics *i.e* extent, cavities and ipsilateral atrophy, revealed no differences between MCAO-vehicle and MCAO-ODN groups, highlighting that ODN treatment was safe when administered from 3 days after the stroke onset (Figure 4, G-I).

Effect of ODN on functional recovery after photothrombotic stroke

Although, intra-arterial MCAO is the most common focal stroke model in the mouse, mimicking malignant infarction, human strokes are mostly small in size. We therefore tested ODN treatment in a photothrombotic model that produces a small cortical infarction. To further differentiate this second model and comply with stroke basic research recommendation (Bernhardt et al., 2017), we used aged female mice (20 ± 2 months). Finally, to further strengthen the translational relevance of our data, we

used a hydrogel impregnated with ODN (0,1 and 5 µg) and performed a single deposition of the hydrogel into the stroke cavity (7.5 µL) 5 days after the onset of stroke (Figure 5A). Photothrombosis produced a well-circumscribed cortical lesion of 3.68 ± 0.43 mm^3 (n = 5 mice) as assessed 2 weeks post-stroke, that resulted in some spontaneous resolution over time with the infarct volume being 2.9 ± 0.66 mm^3 (n = 10 mice) as assessed 6 weeks post-stroke at the completion of the behavioural experiments. Treatment with ODN resulted in a dose-dependent decrease in infarct volume ($F_{(2,40)} = 6.742$; $P < 0.003$: ODN (1 µg), 3.44 ± 0.54 mm^3, and 1.86 ± 0.50 mm^3 for weeks 2 and 6, respectively; ODN (5 µg), 2.73 ± 0.84 mm^3, and 1.51 ± 0.39 mm^3 $P < 0.05$, for weeks 2 and 6, respectively; Figure 5, B and C).

We next tested the mice behaviorally on both the gridwalking (forelimb function) and cylinder (forelimb asymmetry) tasks. Behavioral assessments revealed an increase in the number of footfaults on the gridwalking test (n = 10 per group; Figure 5D) and an increase in spontaneous forelimb asymmetry in the cylinder task (n = 10 per group; Figure 5E) from one-week post-stroke (Clarkson et al., 2010). Treatment with ODN resulted in a dose-dependent decrease in the number of footfaults on the gridwalking task (time effect: $F_{(4,150)} = 33.56$, $P < 0.0001$; treatment effect: $F_{(2,150)} = 28.22$, $P < 0.0001$) and an improvement in forelimb asymmetry in the cylinder task (time effect: $F_{(4,150)} = 48.54$, $P < 0.0001$; treatment effect: $F_{(2,150)} = 18.73$, $P < 0.0001$).

Effects of ODN on modulation of the glial scar

As ODN is a gliopeptide with astrocyte protective feature (Hamdi et al., 2011), we next wanted to investigate whether exogenous administration of ODN has an effect on the glial scar. The glial scar has many roles after a brain ischemia has occurred, both as a regulator of inflammation, but also as a regulator of axonal sprouting and

brain excitability, which are critical processes for cortical remapping (Anderson et al., 2016; Sofroniew, 2015; Clarkson et al., 2010; Brown et al., 2019; Lie et al., 2019). We observed a clear up-regulation in glial fibrillary acidic protein (GFAP) expression in the peri-infarct region at both 2 and 6 weeks post-stroke, with expression levels decreasing the further away from the stroke border we went (Figure 5, F-H). Chronic treatment with ODN resulted in a dose-dependent decrease in the expression of GFAP in the peri-infarct in both layers 2/3 (both 1 µg, $P < 0.001$; and 5 µg, $P < 0.001$), and 5 (only for 5 µg, $P < 0.001$) as assessed 2 weeks post-stroke (Figure 5G). Assessment of GFAP expression in peri-infarct regions 6 weeks post-stroke revealed no differences in expression between vehicle and ODN treated animals in either layers 2/3 or 5 (Figure 5H).

Effects of ODN on tonic inhibitory currents

Given the profile of motor functional recovery we next sort to investigate the changes in tonic inhibitory currents following treatment with ODN. This is also driven by the fact that we have previously reported that tonic inhibitory currents are elevated from 24 h after stroke and remain elevated for extended period of time due in part to the formation of the glial scar (Clarkson et al., 2010; Clarkson et al., 2019; Lie et al., 2019). Tonic inhibitory currents were assessed in the peri-infarct cortex of mice after a photothrombotic stroke to the forelimb motor cortex. Layer 2/3 pyramidal neuron whole-cell voltage-clamp recordings were obtained from brain slices generated *ex vivo* 3-7 days after stroke (Figure 6, A and B). Recordings obtained 3-7 days after stroke showed an increase in $GABA_A$R-mediated tonic inhibition (Control: 53.13 ± 20.04 pA vs. Stroke: 130.90 ± 39.01 pA; $P < 0.001$; Figure 6B). As ODN is released exclusively by astrocytes, extrasynaptic $GABA_A$ receptors are a likely candidate to

mediate its effect on neuronal excitability (Tonon et al., 2019). Therefore, we next examined if bath application of ODN could correct peri-infarct tonic inhibition. Bath application of ODN to slices generated 3-7 days post-stroke resulted in a significant decrease in $GABA_A$R-mediated tonic inhibition (Stroke + ODN: 91.25 ± 13.49 pA; $P < 0.05$; Figure 6B) compared to stroke controls. It should be noted however, that this decrease in tonic inhibitory currents was only a partial reversal with tonic inhibitory currents still significantly elevated compared to sham controls ($P < 0.05$).

Discussion

Studies over recent years have shown that the peri-infarct cortex, which is the tissue adjacent to the stroke, is in a state of heightened plasticity during the sub-acute period (Murphy and Corbett, 2009). The process of plasticity is highly influenced by $GABA_AR$ signaling and tonic inhibition, which maintains and shapes the level of neuronal excitability (Raimondo *et al.*, 2017). Alteration in GABAergic signaling has been previously reported to be triggered by stroke in both animals and humans (Carmichael 2012; Johnstone *et al.* 2018). Accordingly, dampening tonic inhibitory currents using a NAM targeting α_5-containing $GABA_ARs$ from 3-7 days post-stroke, but not acutely within hours, increases motor functional recovery in animal stroke models (Clarkson et al., 2010; Lake et al., 2015). Consistent with these observations, the present findings demonstrate that exogenous administration of ODN enhances cortical excitability in a magnitude that makes it toxic when administered during the acute stage of stroke (within hours of stroke onset), however, makes it instrumental to safely boost functional recovery when administered during the sub-acute (3-7 days) recovery stages of stroke.

The endozepine, ODN, has been repeatedly categorized as a $GABA_AR$ NAM (Bormann et al., 1985; Costa and Guidotti, 1991; Alfonso *et al.,* 2012; Dumitru et al., 2017). Yet, all these experiments have been conducted *in vitro*. Here, we report for the first time, *in vivo,* that ODN increases cortical neuronal activity and excitability. Interestingly, we also report that astrocytes respond to the treatment. The question of whether this activation is a consequence of neuronal activity or a direct effect on astrocytes, as we previously report in cell culture, remains unclear (Gach et al., 2015). However, it is possible that ODN works on both systems as we report herein

that administration of ODN partially dampens both the stroke-induced elevation in tonic inhibitory currents as well as the level of reactive astrogliosis in the peri-infarct cortex.

Capitalizing upon our confirmation of ODN as an enhancer of cortical excitability we assessed the effect of a gain or loss of ODN during the acute phase of brain ischemia/reperfusion. In line with our predictions, when ODN was administrated during brain ischemia, cerebral damage was dramatically increased. In addition, the finding that $DBI^{-/-}$ mice were less vulnerable to transient focal ischemia than wild-type mice, suggests that even the endogenous production of DBI (and therefore ODN) during stroke, is deleterious.

In stroke, minor changes in various physiological and metabolic parameters can have major consequences on tissue viability. We verified that i.c.v administration of ODN did not change body temperature, food intake or cardiovascular activity. Therefore, the most parsimonious explanation for why ODN exacerbated the cellular damage following stroke is due to an increase in neuronal excitability. The propagation of waves of spreading depolarizations out from the site of infarction is known to be a leading cause of ischemic infarct growth (Chuquet *et al.,* 2007; Hartings *et al.,* 2017, von Bornstädt *et al.,* 2015). We report here that the pro-excitotoxic effect of ODN contributes to an increase in spreading depolarizations, which for neurons at immediate threat of death means that ODN may amplify the depolarization and lead to an irreversible calcium overload. Our results indicate that there is a need to develop specific endozepine blockers to prevent their action on $GABA_A$Rs during the acute phase of cerebral ischemia.

To date, no NAMs that target the benzodiazepine-binding site to reduce GABAergic activity and that lack any pro-convulsant or anxiogenic effects are available for clinical use. However, clinical trials using α5-containing $GABA_AR$ NAMs for enhancing stroke recovery are being explored in phase II trials (ClinicalTrials.gov ID: Hoffman La-Roche - NCT02928393; Servier RESTORE BRAIN Study - NCT02877615). It is increasingly recognized that GABAergic NAMs used at a safe dosage and that target specific subunit compositions, will be therapeutically useful; for example, to improve cognitive functions in brain conditions where diminished excitability has to be boosted (Bolognani *et al.,* 2015; Soh and Lynch, 2015). There is also growing evidence that impairment in GABA transporter (GAT-3/GAT-4) function contributes to the peri-infarct zone changes in neuronal inhibition and post-stroke functional recovery (Clarkson et al., 2010, Carmichael, 2012). As a consequence, the excessive GABAergic tone inhibits sensorimotor recovery and is likely due in part to synaptic plasticity and long-term potentiation (LTP), being sub-optimal (Atack *et al.,* 2006). Two independent studies have demonstrated that the use of a benzodiazepine-site specific NAM improves post-stroke motor recovery (Clarkson *et al.,* 2010; Lake *et al.,* 2015). In addition, a recent study showed that the treatment with the GAT3 substrate, L-isoserine, administered directly into the stroke cavity, can increase GAT3 expression and improve functional recovery after focal ischemic stroke (Lie et al., 2019). Following this idea and protocol, we found that daily administration of ODN started 3 days after ischemia or hydrogel delivery from 5 days (*i.e*. when the risk of ODN induced cell death had ceased) remarkably improved motor coordination. Of note, the precursor of ODN, DBI, is one of the most transcripted genes in astrocytes (Zhang et al., 2014). The fact that GABA inhibits the release of ODN by astrocytes (Patte et al., 1999), suggests that in the neighbourhood

of the stroke lesion, the excess in ambient GABA is likely preventing sufficient endozepine production.

This functional recovery cannot be due to a difference in stroke severity between groups because *i)* the average decrease of blood flow was identical over the 60 minutes of ischemia, *ii)* the mean brain histological sequelae were similar at day 28 and *iii)* mortality rate had the same kinetics in both groups. Moreover, ODN treated animals did not display any obvious behavior indicative of anxiety, aggression or hyperactivity suggesting that both the timing and dose of ODN administered led to a safe and efficient treatment to promote delayed functional recovery.

To date, all translational studies have failed to treat stroke. Several recommendations have been made, among which were the use of aged animals of both sex since aging remains the major non-modifiable risk factor for stroke (Jolkkonen and Kwakkel 2016; Corbett et al., 2017). Moreover, although the intra-arterial filament occlusion is the gold-standard model for pre-clinical investigation, it results in a large corticostriatal infarction that, when transposed in human, would be fatal or with low potential of recovery. Therefore, to increase the translational value of our results, we studied the efficiency of ODN in another paradigm. Using the photothrombotic model of ischemia in aged female mice, we obtained a small infarction circumscribed to the cortex. We took advantage of the topology of the lesion to also test whether a single depot of ODN into the infarction cavity on day 5 post-stroke would improve functional recovery. Although the number of new peptides entering clinical trials continues to grow, their therapeutic potential in neurology has not yet been realized because they rarely get through the blood-brain-barrier and their half-life *in vivo* limits the time window to exert their action (Penchala et al., 2015). Hydrogel-impregnated with ODN

provides a protective micro-environment for peptides and allows controlled delivery around the lesion, where excitability need to be enhanced. In this second stroke model, ODN was able to improve sensory-motor task performance as soon as week 1. These studies highlight a novel example for hydrogel delivery systems offering a support for effective peptide biodisponibility that bypasses the blood-brain-barrier to achieve consistent recovery post-stroke.

Overall, our data are strikingly reminiscent of the findings of Clarkson *et al.,* 2010 and Lake *et al.,* 2015. Using a small naturally occurring peptide that is expressed and released by astrocytes and known to act as a $GABA_AR$ NAM, we found the same versatile effect in stroke as with the synthetic $GABA_AR$ NAM, L655-708. This imidazobenzodiazepine is selective for the extrasynaptic $GABA_AR$ that contains the benzodiazepine sensitive subunit α_5 and, as an inverse agonist, reduces the tonic inhibition mediated by these $GABA_AR$. Interestingly, L655-708 has been shown to facilitate LTP by shifting toward less inhibitory activity (Atack *et al.,* 2006). Similarly, we found that ODN was able to dampen the ambient tonic inhibition surrounding the stroke lesion. This disinhibition may be permissive for plastic rearrangements in the peri-infarct cortex to occur (Ziemann et al. 2001; Cicinelli et al., 2003; Clarkson and Carmichael, 2009). Therefore, one hypothesis requiring future attention is that ODN selectively binds to α_5 containing $GABA_AR$. It is also possible that these changes in tonic inhibitory currents could be occurring through changes in presynaptic GABA signalling or astrocytic function, which is another two suggested pathways that need to be explore in furture experiments.

The modification of network connections and synaptic strength allowing functional recovery require that homeostatic mechanisms, such as the maintenance of

excitation/inhibition balance at the network, single cell and synapse level, be in their operating range (Buzsáki, 2007). Our results suggest that endozepines play a significant role to tuning this balance and reinforce the idea that an appropriate correction of GABAergic tone at the right time can facilitate functional recovery after stroke.

Methods

Animals

For these studies, 8-12 week old (20-25 g) male C57BL/6J mice were purchased from Janvier Laboratories. ACBP knockout ($ACBP^{-/-}$ hereinafter referred to as $DBI^{-/-}$) mice were obtained from Prof. S. Mandrup Laboratory (University of Southern Denmark), bred as previously described (Neess et al., 2011) and backcrossed to a Bl/6JBom background. Aged female (20 ± 2 months) mice were obtained from the Hercus Taieri Resource Unit at the University of Otago.

In vivo electrophysiology

Under isoflurane anesthesia (2-2.5%) two small holes were drilled over the whisker barrel cortex with the dura matter intact and two glass micropipettes were inserted (one for the recording and one for the micro-injection). After the surgical procedure isoflurane was reduced to 1.1 ± 0.1% for a resting period of 30-45 min followed by the recording period. All *in vivo* recordings were done in a Faraday chamber and used an amplifier PowerLab 8/35 (AD-Instrument). Raw data were aquired with Labchart software (AD Instrument).

Local field potential (LFP) and extracellular unit (EU) recording. An ACSF-filled glass-micropipette/AgCl/Ag electrode, 3-6 µm diameter opening, was positioned in cortical layer 4 of the whisker barrel cortex. Reference and ground electrodes (AgCl/Ag wire) were inserted into the cerebellum. For ODN microinjection, a second glass micropipette (10 µm diameter opening) was placed 50-100 µm away from the tip of the recording pipette. For KCl-induced spreading depolarization waves, 2 µL of KCl (0.5 mol/L) was slowly infused (10 minutes) at a distant site from the recording site (4

mm). The signal was bandpass filtered at 200-2000 Hz and digitized at 20 kHz for EU or at 1-100 Hz and digitized at 1kHz for LFP. Signals were recorded for 12 min before the intracortical microinjection of 1 µg of ODN (0.5 µL) and compared to a 12 min period beginning 3 min after the end of the microinjection (3 min). Spikes detection and sorting was then performed semi-automatically, using Klusta software suite (Rossant et al., 2016), freely available on the Web (http://klusta-team.github.io).

Somatosensory evoked potentials (SEP). The whiskers on the left of the animal's snout were stimulated with a short rod controlled by an Arduino UNO board (open-source microcontroller) once every 10 s, repeated 100 times. Signal was bandpass filtered between 1 and 100 Hz and digitized at 4 kHz. Data analysis was performed by a custom-made script in MATLAB (The MathWorks). For the slope of SEP, 100 trials were superimposed and averaged; the initial deflection of the LFP was defined as the interval within 20–80% of the peak-to-peak amplitude. The slope was computed by linear regression of the selected region.

Intravital calcium imaging

A cranial window was made over the somato-sensory cortex as previously described (Chuquet et al, 2010). Imaging was performed under anesthesia using 2-photon laser scanning microscope (SP8, Leica). SR-101 (1µM applied on the cortex for 10 min) and OGB1-AM (1.2µg in 1 µL micro-injected in the somatosensory cortex) were both excited at 805 nm. Frames (256 × 256 pixels) were collected at a frequency of 3 Hz. X-y drift where automatically corrected off-line. All traces where median filtered. Signal was expressed as relative OGB1-AM fluorescence changes (dF/F_0) where F_0 is the mean of the lowest 20% of the somatic fluorescence signals. Astrocytic calcium surges were defined as transient increase of dF/F_0 signal exceeding 3 SDs.

Stroke models

*Middle cerebral artery occlusion***.** Temporary focal cerebral ischemia was induced under general anesthesia (isoflurane 1.5-2%) by occlusion of the right middle cerebral artery (MCAO) by the means of the intraluminal filament technique. Briefly, a nylon thread (80 µm in diameter) with a distal cylinder (1.5 mm and 180 µm in diameter) was inserted into the common carotid artery, advanced to the origin of the MCA and removed 60 minutes later to allow reperfusion. A laser-Doppler flowmetry probe (Moor Instruments) was used to continuously monitor CBF. For sham-operated animals, the nylon thread was not pushed to the origin of the MCA. Post-surgery analgesic care comprised intradermal injection of ropivacaine (25 µL at 2.5 mg/mL, Naropeine) around sutures and local applications of lidocaine/prilocaine mixture cream (2,5% EMLA, AstraZeneca). The animals were then allowed to recover and were killed 48 hours or at day 28 after MCAO.

Cortical photothrombosis. Focal stroke was induced in the left hemisphere using the photothrombosis method in aged (20 ± 2 month old) female C57BL/6J mice weighing 35.8 ± 5.6 g (Clarkson et al., 2010; Clarkson et al, 2011; Clarkson et al., 2019). Briefly, under isoflurane anesthesia (2-2.5% in O_2) mice were placed in a stereotactic apparatus, the skull was exposed through a midline incision, cleared of connective tissue and dried. A cold light source (KL1500 LCD, Zeiss) attached to a 40x objective giving a 2 mm diameter illumination was positioned 1.5 mm lateral from Bregma and 0.2 mL of Rose Bengal solution (Sigma; 10g/L in normal saline, i.p.) was administered. After 5 min the brain was illuminated through the intact skull for 15 min. Mice were housed under a 12-hour light/dark cycle with *ad libitum* access to food and water.

All animals were randomly assigned to a treatment group 5 days post-stroke, by an operater not undertaking behavioral or post-hoc histological or immunohistochemical assessments. All assessments were carried-out by observers blind as to the treatment group.

NMDA-induced excitotoxic damage

In isoflurane-anesthetized mice, excitotoxic lesions were induced by NMDA micro-injection (20 nmol/0.5 µL) into the right striatum (2.5 mm lateral, -4.0 mm ventral and -0.7 mm posterior to the Bregma) infused at a rate of 0.2 µL/min. The lesion volume was quantified 48 hours later.

Peptide synthesis, drugs and hydrogel preparation

Mouse/rat ODN (H-Gln-Ala-Thr-Val-Gly-Asp-Val-Asn-Thr-Asp-Arg-Pro-Gly-Leu-Leu-Asp-Leu-Lys-OH) was synthesized as previously described (Leprince *et al*., 2001). Flumazenil, a selective antagonist of the benzodiazepine-site of the $GABA_AR$ and NMDA were purchased from Sigma-Aldrich and dissolved in sterile HEPES buffer supplemented with KCl (2.5 mmol/L) and NaCl (145 mmol/L) pH 7.4 and DMSO (dilution 1:4) for flumazenil. ODN or its vehicle was infused over 5 minutes into the lateral ventricle (3 µL; -0.1 mm posterior, 0.8 mm lateral, -2.5 mm ventral to the Bregma) or into the *cisterna magna* for the experiment conducted under the 2-photon microscope.

***In vivo* dosing with hydrogel impregnated with ODN**

A hyaluronan/heparan sulfate proteoglycan biopolymer hydrogel (HyStem-C, BioTime, Inc.) was employed to locally deliver ODN or saline (vehicle control), to the peri-infarct cortex as described previously (Clarkson et al., 2011; Houlton et al.,

2019). In prior studies, we have reliably shown that hydrogels can be used to release small and large proteins for at least 3 weeks from the stroke cavity (Overman et al., 2012; Clarkson et al., 2011; Li et al., 2010). Five days after stroke, 7.5 μL of HyStem-C, impregnated with either ODN (1 μg or 5 μg) or saline-vehicle was injected directly into the stroke infarct cavity using a 30-gauge needle attached to a Hamilton syringe. HyStem-C was prepared according to the manufacturer's instructions. In brief, ODN or saline was added to the HyStem/Gelin-S mix (component 1 of hydrogel), followed by addition of Extralink (component 2 of hydrogel) in a 4:1 ratio. The impregnated HyStem-C mix was injected immediately after preparation into the stroke cavity at stereotaxic coordinates 0 mm AP, 1.5 mm ML, and 0.75 mm DV.

Behavioral tests

*Middle cerebral artery occlusion***.** Behavioral tests were conducted by a manipulator who was blinded to treatment groups. After a pre-test performed 3 or 4 days before MCAO surgery, 2 tests (3 tasks) were conducted once a week in between day 3 and 28 post-occlusion.

The *pole test* was performed as described by Matsuura *et al.,* 1997, with minor modifications. The test apparatus consisted of a vertical pole (55 cm) covered with tape (Durapore, 3M) to create a rough surface. Mice performed two different tasks. First, they were placed head upward on the top of the pole. The time the mouse took to turn completely head downward was measured (*return task*). The second part of the test consisted in the descent to the floor with its front paws (*descent task*). The third test was the *beam crossing* test (Carter *et al.,* 2001), measuring the time for a mouse to cross a horizontal beam (diameter: 10 mm; length: 1 m). For animals unable to perform one of these 3 tasks, a time penalty of 60, 60 and 200 s was

respectively attributed, corresponding to the worst accomplished performances recorded in our conditions (Mann and Chesselet, 2014). Each test was repeated 5 times (*pole test*) or 3 times (*beam crossing* test) and the average time was calculated.

*Cortical photothrombosis***.** Recovery of forelimb motor function following a photothrombotic stroke was determined by the cylinder and grid-walking tasks to assess their exploratory behavior and walking, respectively, as previously reported (Clarkson et al., 2010). The mice were tested approximately 7 days prior to stroke to establish a baseline performance level and then after 7, 14, 28 and 42 days post-stroke at approximately the same time each day. Observers blinded to the treatment group scored behaviors as previously described (Clarkson et al., 2010).

Immunofluorescent labeling of GFAP and infarct volume

Reactive astrogliosis was assessed by immunofluorescent labelling for GFAP at 2 and 6 weeks post-stroke. Brains were sectioned and every sixth section (30 μm thick) was collected through the stroke and stored in cryopreservation solution until used. Sections were rinsed in tris buffered saline (TBS) and transferred to 0.76% glycine in TBS for 10 min at room temperature, followed by a second TBS rinse. The sections were blocked for 60 min in TBS containing 5% donkey serum with 0.3% Triton X-100 before being incubated in TBS with 2% donkey serum and 0.3% Triton X-100 containing the primary antibody (chicken anti-mouse GFAP, 1:3,000, AB5541, Millipore) for 48 hours at 4°C. Following incubation in primary antibody, sections were washed three times in TBS followed by incubation for 2 hours at RT in TBS with 2% normal donkey serum and 0.3% Triton X-100 containing the fluorescent secondary antibody (anti-chicken Alexa-488, 1:1,000, SA5-10071, ThermoFisher Scientific)

followed by the nuclear counter stain Hoechst (1:1,000, Sigma-Aldrich) in TBS for 5 min at RT. Images were taken with an Olympus BX61 microscope, and two sections from each animal were included in the analysis. Changes in GFAP staining was investigated 2 and 6 weeks post-stroke, with measurements taken 0-200 μm and 800-1000 μm from the stroke border in layers 2/3 and 5. Using the software FIJI Image J (National Institutes of Health, USA) the integrated density value (IDV) was measured in all 4 regions of interest (ROIs) in the green channel for GFAP.

Infarct volumes were determined 2 and 6 weeks post-stroke using cresyl violet staining and Image J analysis (Clarkson et al. 2010). The analysis is based on obtaining measurements from every sixth section through the entire infarct (area in mm^2), and infarct volume was quantified as follows: infarct volume (mm^3) = areas (mm^2) x (section thickness (mm) + section interval (mm)). All analyses were performed by an observer blind to the treatment groups.

Whole-cell voltage-clamp electrophysiological recordings

For recordings from layer 2/3 pyramidal neurons in sham or stroke mice, strokes were induced in 2-3 month-old-mice. The mice were anesthetized with isoflurane and brains isolated at 3-7 days post-stroke or sham surgery and prepared for recordings of tonic currents (Clarkson et al., 2010; Clarkson et al., 2019). All recordings were made from peri-infarct cortical layer 2/3 pyramidal neurons within the primary motor cortex, as previously described (Clarkson et al., 2010; Clarkson et al., 2019). Neurons were voltage-clamped in whole-cell configuration using a MultiClamp-700B amplifier using microelectrodes (3–5 MΩ) filled with a cesium-methyl-sulfonate ($CsMeSO_4$)-based internal pipette solution. The recording aCSF was supplemented

with 5 µM GABA to replenish the extracellular GABA concentration reduced by the high-flow perfusion of the slices.

Tonic inhibotry currents (I_{tonic}) were recorded as the reduction in baseline holding currents (I_{hold}) after bath-applying a saturating amount (100 µM) of the $GABA_AR$ antagonist SR-95531 (gabazine), while voltage-clamping at +10 mV. ODN was added to the recording aCSF *via* perfusion and their effects on I_{tonic} were recorded as the post-drug shift in I_{hold}. Drug perfusion was continued until the shifting I_{hold} remained steady for 1-2 min. Gabazine and ODN were dissolved in H_2O. All analyses were performed by an investigator blinded to the treatment condition.

Statistics

Data are presented as mean ± SEM or as box-and-whisker plot showing the median (box = first and third quartiles; whisker = range). All statistics were performed using Prism software (Graphpad). Normal distribution of the datasets was tested by a Kolmogorov-Smirnov test. A paired Student's *t*-test was used for pairwise means comparisons. A Mann–Whitney test was used for pairwise means comparisons of data that did not follow normal distribution. For recovery studies, two-way ANOVA followed by post-hoc Tukey's or Bonferonni's test for multiple comparisons was performed.

Study approval

Experiments, approved by the Ethics Committee for Animal Research of Normandy or the University of Otago Animal Ethics Committee, were conducted by authorized investigators in accordance with the recommendations of the European Communities

86/609/EEC. All procedures were undertaken and reporting done in accordance to the ARRIVE (Animal Research: Reporting *In Vivo* Experiments) guidelines.

Author contributions: R.L. performed surgeries (MCAO, electrophysiology and 2-photon cranial window) behavioral tests, analysed data and planned the experiments; M.H. developed and performed *in vivo* electrophysiology; J.M. performed MCAO on DBI KO mice: E.K.G. performed the surgeries, behavioral tests and immunohistochemistry for the hydrogel-ODN stroke study; R.Y.N. performed the patch-clamp electrophysiology studies; P.Q. and K.L. conceived and developed the custom Matlab routines for electrophysiology data analysis. B.L. and J.L. synthetized the peptide; K.G. contributed to the development of calcium imaging in the first part of the project. A.B.M and S.M. developed and provided the DBI KO mice; A.N.C. designed and supervised the hydrogel-ODN stroke study, helped collect and analysed the data and contributed to writing the manuscript; D.V. and J.L. coordinated and secured funding for the project and provided resources and expertise for the research; J.C. conceived and supervised the experiments, analysed data and wrote the manuscript. The manuscript was reviewed and edited by all authors.

Acknowledgement: We thank Dr Arnaud Arabo who provided help and expertise that greatly assisted the research.

Sources of Funding: This research was supported by the *Institut National de la Santé et de la Recherche Médicale* U1239, The *fondation pour la recherche sur les AVC*, Normandy Region and the European Union. Europe gets involved in Normandy with European Regional Development Fund (ERDF). This work was also supported by the New Zealand Neurological Foundation, a Royal Society of New Zealand

Project Grant, funding from the Ministry of Business, Innovation and Employment, New Zealand, Brain Research New Zealand for animal costs and an equipment grant from the New Zealand Lottery Health.

References

Alfonso J, Le Magueresse C, Zuccotti A, Khodosevich K, Monyer H. Diazepam binding inhibitor promotes progenitor proliferation in the post-natal SVZ by reducing GABA signaling. *Cell Stem Cell*. 2012;10:76–87.

Alia C, Spalletti C, Lai S, Panarese A, Micera S, Caleo M. Reducing $GABA_A$-mediated inhibition improves forelimb motor function after focal cortical stroke in mice. *Sci Rep*. 2016;6:37823.

Anderson MA, et al. Astrocyte scar formation aids central nervous system axon regeneration. *Nature*. 2016;532:195–200.

Atack JR, Bayley PJ, Seabrook GR, Wafford KA, McKernan RM, Dawson GR. L-655,708 enhances cognition in rats but is not proconvulsant at a dose selective for alpha5-containing $GABA_A$ receptors. *Neuropharmacology*. 2006;51:1023–1029.

Bachtiar V, Stagg CJ. The role of inhibition in human motor cortical plasticity. *Neurosci*. 2014;278:93–104.

Barmack NH, Bilderback TR, Liu H, Qian Z, Yakhnitsa V. Activity-dependent expression of acyl-coenzyme a-binding protein in retinal Müller glial cells evoked by optokinetic stimulation. *J Neurosci*. 2004;24:1023–1033.

Bernhardt J, et al. Agreed definitions and a shared vision for new standards in stroke recovery research: the stroke recovery and rehabilitation roundtable taskforce. *Neurorehabil Neural Repair*. 2017;31:793–799.

Bolognani F, et al. RG1662, a selective $GABA_A$ α5 receptor negative allosteric modulator, increases gamma power in young adults with down syndrome. *Neurol*. 2015;84: sup. abst. P6.273.

Bormann J, Ferrero P, Guidotti A, Costa E. Neuropeptide modulation of GABA receptor C1-channels. *Regul Pept*. 1985;4:33–38.

Bormann J. Electrophysiological characterization of diazepam binding inhibitor (DBI) on $GABA_A$ receptors. *Neuropharmacology*. 1991;30:1387–1389.

Brown CE, Aminoltejari K, Erb H, Winship IR, Murphy TH. In vivo voltage-sensitive dye imaging in adult mice reveals that somatosensory maps lost to stroke are replaced over weeks by new structural and functional circuits with prolonged modes of activation within both the peri-infarct zone and distant sites. *J Neurosci*. 2009;29:1719–1734.

Buzsáki G; Buzsáki G, ed. Rhythms of the brain, New York, New York: Oxford University Press; 2007.

Carmichael ST. Brain excitability in stroke: the yin and yang of stroke progression. *Arch Neurol*. 2012;69:161–167.

Carter RJ, Morton J, Dunnett SB. Motor coordination and balance in rodents. *Curr Protoc Neurosci*. 2001;8:8–12.

Chuquet J, Hollender L, Nimchinsky EA. High-resolution in vivo imaging of the neurovascular unit during spreading depression. *J Neurosci*. 2007;27:4036–4044.

Chuquet J, Quilichini P, Nimchinsky EA, Buzsáki G. Predominant enhancement of glucose uptake in astrocytes versus neurons during activation of the somatosensory cortex. *J Neurosci*. 2010;30:15298–15303.

Cicinelli P, Pasqualetti P, Zaccagnini M, Traversa R, Oliveri M, Rossini PM. Interhemispheric asymmetries of motor cortex excitability in the postacute stroke stage: a paired-pulse transcranial magnetic stimulation study. *Stroke*. 2003;34:2653–2658.

Clarkson AN, Carmichael ST. Cortical excitability and post-stroke recovery. *Biochem Soc Trans*. 2009;37:1412–1414.

Clarkson AN, Huang BS, Macisaac SE, Mody I, Carmichael ST. Reducing excessive GABA-mediated tonic inhibition promotes functional recovery after stroke. *Nature*. 2010;468:305–309.

Clarkson AN, Parker K, Nilsson M, Walker FR, Gowing EK. Combined ampakine and BDNF treatments enhance poststroke functional recovery in aged mice via AKT-CREB signaling. *J Cereb Blood Flow Metab*. 2015;35:1272–1279.

Clarkson AN, Overman JJ, Zhong S, Mueller R, Lynch G, Carmichael ST. AMPA receptor-induced local brain-derived neurotrophic factor signaling mediates motor recovery after stroke. *J Neurosci*. 2011;31:3766–3775.

Clarkson AN et al. The flavonoid, 2'-methoxy-6-methylflavone, affords neuroprotection following focal cerebral ischaemia. J Cereb Blood Flow Metab. 2019;39:1266–1282.

Corbett D, et al. Enhancing the Alignment of the Preclinical and Clinical Stroke Recovery Research Pipeline: Consensus-Based Core Recommendations From the Stroke Recovery and Rehabilitation Roundtable Translational Working Group. *Neurorehabil Neural Repair*. 2017;31:699–707.

Costa E, Guidotti A. Diazepam binding inhibitor (DBI): A peptide with multiple biological actions. *Life Sci*. 1991;49:325–344.

Dumitru I, Neitz A, Alfonso J, Monyer H. Diazepam Binding Inhibitor promotes stem cell expansion controlling environment-dependent neurogenesis. *Neuron*. 2017;94:125–137.

Ferrero P, Santi MR, Conti-Tronconi B, Costa E, Guidotti A. Study of an octadecaneuropeptide derived from diazepam binding inhibitor (DBI): biological activity and presence in rat brain. *Proc Natl Acad Sci U S A*. 1986;83:827–831.

Gach K, et al. Detection, characterization and biological activities of [bisphospho-Thr3,9]ODN, an endogenous molecular form of ODN released by astrocytes. *Neurosci*. 2015;290:472–484.

Galeffi F, Sinnar S, Schwartz-Bloom RD. Diazepam promotes ATP recovery and prevents cytochrome C release in hippocampal slices after in vitro ischemia. *J Neurochem*. 2000;75:1242–1249.

Green AR, Hainsworth AH, Jackson DM. GABA potentiation: a logical pharmacological approach for the treatment of acute ischaemic stroke. *Neuropharmacology*. 2000;39:1483–1494.

Guidotti A, Forchetti CM, Corda MG, Konkel D, Bennett CD, Costa E. Isolation, characterization, and purification to homogeneity of an endogenous polypeptide with agonistic action on benzodiazepine receptors. *Proc Natl Acad Sci USA*. 1983;80:3531–3535.

Hamdi Y, et al. Protective effect of the octadecaneuropeptide on hydrogen peroxide-induced oxidative stress and cell death in cultured rat astrocytes. *J Neurochem*. 2011;118:416–428.

Hartings JA, et al. The continuum of spreading depolarizations in acute cortical lesion development: Examining Leão's legacy. *J Cereb Blood Flow Metab*. 2017;37:1571–1594.

Houlton J, Zhou LYY, Barwick D, Gowing EK, Clarkson AN. Stroke induces a BDNF-dependent improvement in cognitive flexibility in aged mice. [published online ahead of print May 5th, 2019]. *Neural Plasticity* doi: 10.1155/1460890.

Hummel FC, et al. Deficient intracortical inhibition (SICI) during movement preparation after chronic stroke. *Neurol*. 2009;72:1766–1772.

Johnstone A, Levenstein JM, Hinson EL, Stagg CJ. Neurochemical changes underpinning the development of adjunct therapies in recovery after stroke: A role for GABA? *J Cereb Blood Flow Metab*. 2018;38:1564–1583.

Jolkkonen J, Kwakkel G. Translational hurdles in stroke recovery studies. *Transl Stroke Res*. 2016;7:331–342.

Kim YK, Yang EJ, Cho K, Lim JY, Paik NJ. Functional recovery after ischemic stroke is associated with reduced GABAergic inhibition in the cerebral cortex: a GABA PET study. *Neurorehabil Neural Repair*. 2014;6:576–583.

Lake EM, et al. The effects of delayed reduction of tonic inhibition on ischemic lesion and sensorimotor function. *J Cereb Blood Flow Metab*. 2015;35:1601–1609.

Leprince J, et al. Synthesis, conformational analysis and biological activity of cyclic analogs of the octadecaneuropeptide ODN. Design of a potent endozepine antagonist. *Eur J Biochem*. 2001;268:6045–6057.

Li S et al. An age-related sprouting transcriptome provides molecular control of axonal sprouting after stroke. *Nat Neurosci*. 2010;13:1496–504.

Lie ME, et al. GAT3 selective substrate l-isoserine upregulates GAT3 expression and increases functional recovery after a focal ischemic stroke in mice. *J Cereb Blood Flow Metab*. 2019;39:74–88.

Loomis WF, Behrens MM, Williams ME, Anjard C. Pregnenolone sulphate and cortisol induce secretion of acyl-CoA-binding protein and its conversion into endozepines from astrocytes. *J Biol Chem*. 2010;285:21359–21365.

Mann A, Chesselet MF. Techniques for motor assessment in rodent. LeDoux M ed. *Movement disorders, genetics and models* 2nd edition, Elsevier Academic Press, 2014:139–157.

Marshall JW, Green AR, Ridley RM. Comparison of the neuroprotective effect of clomethiazole, AR-R15896AR and NXY-059 in a primate model of stroke using histological and behavioural measures. *Brain Res*. 2003;972:119–126.

Matsuura K, Kabuto H, Makino H, Ogawa N. Pole test is a useful method for evaluating the mouse movement disorder caused by striatal dopamine depletion. *J Neurosci Methods*. 1997;73:45–48.

Möhler H. Endogenous benzodiazepine site peptide ligands operating bidirectionally in vivo in neurogenesis and thalamic oscillations. *Neurochem Res*. 2014;39:1032–1036.

Murphy TH, Corbett D. Plasticity during stroke recovery: from synapse to behaviour. *Nat Rev Neurosci.* 2009;10:861–72.

Neess D, et al. Disruption of the acyl-CoA binding protein gene delays hepatic adaptation to metabolic changes at weaning. *J Biol Chem*. 2011;286:3460–3472.

Orfila JE, et al. Delayed inhibition of tonic inhibition enhances functional recovery following experimental ischemic stroke. *J Cereb Blood Flow Metab*. 2019;39:1005–1014.

Overman JJ et al. A role for ephrin-A5 in axonal sprouting, recovery, and activity-dependent plasticity after stroke. *Proc Natl Acad Sci U S A*. 2012;109:2230–2239.

Patte C, et al. GABA inhibits endozepine release from cultured rat astrocytes. *Glia*. 1999;25:404–411.

Penchala SC, et al. A biomimetic approach for enhancing the in vivo half-life of peptides. *Nat Chem Biol*. 2015;10:793–798.

Qian Z, Bilderback TR, Barmack NH. Acyl coenzyme A-binding protein (ACBP) is phosphorylated and secreted by retinal Müller astrocytes following protein kinase C activation. *J Neurochem*. 2008;4:1287–1299.

Raimondo JV, Richards BA, Woodin MA. Neuronal chloride and excitability - the big impact of small changes. *Curr Opin Neurobiol*. 2017;43:35–42.

Rossant C, et al. Spike sorting for large, dense electrode arrays. *Nat Neurosci*. 2016;19:634–641.

Roux L, Buzsáki G. Tasks for inhibitory interneurons in intact brain circuits. *Neuropharmacology*. 2015;88:10–23.

Schwartz RD, Huff RA, Yu X, Carter ML, Bishop M. Post-ischemic diazepam is neuroprotective in the gerbil hippocampus. *Brain Res*. 1994;647:153–160.

Schwartz RD, Yu X, Katzman MR, Hayden-Hixson DM, Perry JM. Diazepam, given post-ischemia, protects selectively vulnerable neurons in the rat hippocampus and striatum. *J Neurosci*. 1995;15:529–539.

Schwartz-Bloom RD, Sah R. Gamma-aminobutyric acid (A) neurotransmission and cerebral ischemia. *J Neurochem*. 2001;77:353–371.

Schwartz-Bloom RD, McDonough KJ, Chase PJ, Chadwick LE, Inglefield JR, Levin ED. Long-term neuroprotection by benzodiazepine full versus partial agonists after transient cerebral ischemia in the gerbil. *J Cereb Blood Flow Metab*. 1998;18:548–558.

Shuaib A, Kanthan R. Amplification of inhibitory mechanisms in cerebral ischemia: an alternative approach to neuronal protection. *Histol Histopathol*. 1997;12:185–194.

Sofroniew MV. Astrocyte barriers to neurotoxic inflammation. *Nat Rev Neurosci*. 2015;16:249–263.

Soh MS, Lynch JW. Selective modulators of α5-containing $GABA_A$ receptors and their therapeutic significance. *Curr Drug Targets*. 2015;16:735–746.

Sydserff SG, Cross AJ, Green AR. The neuroprotective effect of chlormethiazole on ischaemic neuronal damage following permanent middle cerebral artery ischaemia in the rat. *Neurodegeneration*. 1995;4:323–328.

Tonon MC, et al., Endozepines and their receptors: Structure, functions and pathophysiological significance. [published online ahead of print July 5th, 2019] *Pharmacol Ther*. doi: 10.1016/j.pharmthera.

Vezzani A, Serafini R, Stasi MA, Samanin R, Ferrarese C. Epileptogenic activity of two peptides derived from diazepam binding inhibitor after intrahippocampal injection in rats. *Epilepsia*. 1991;32:597–603.

von Bornstädt D, et al. Supply-demand mismatch transients in susceptible peri-infarct hot zones explain the origins of spreading injury depolarizations. *Neuron*. 2015;85:1117–11131.

Zhang Y, et al. An RNA-sequencing transcriptome and splicing database of glia, neurons, and vascular cells of the cerebral cortex. *J Neurosci*. 2014;34:11929–11947.

Ziemann U, Muellbacher W, Hallett M, Cohen LG. Modulation of practice-dependent plasticity in human motor cortex. Brain. 2001:24:1171–1181.

Legends to figures

Figure 1. The gliopeptide ODN enhances neuronal and astrocytic activity in the cortex *in vivo*. A, Experimental arrangement showing pipette-positions for microinjection of ODN in the vicinity (~100 µm) of the recording pipette (layer 4). **B**, Representative extracellular unit recording trace comparing spontaneous neuronal spiking activity before and after ODN infusion. The post-treatment period recording started 6 min after the start of the infusion. The occurrence of spikes is depicted by short black bars underneath the trace. **C**, The infusion of the vehicle solution did not change spiking frequency ($P > 0.05$ vs. pre-vehicle period, n = 6 mice). ODN significantly increased spiking ($P < 0.05$ vs. pre-ODN period, n = 6 mice). **D**, Experimental set-up for sensory evoked potential (SEP) recorded in the whisker

barrel cortex. The contralateral whisker pad was mechanicaly stimulated every 10 s evoking the typical negative shift of the LFP trace (**E)**. **F**, Representative SEP obtained after the average of 100 stimulations. **G**, The SEP slope of the control group remained unchanged after the infusion of vehicle ($P > 0.05$, pre- vs. post-treatment, n = 6 animals) whereas ODN treatment significantly increased the SEP slope ($P < 0.05$, pre- vs. post-treatment, n = 6 animals). **H,** Experimental set-up for 2-photon imaging of astrocyte activity. ODN or its vehicle was administered by the cisterna-magna route. **I**, Astrocytes (white arrowheads) were double-labeled with Ca^{2+} -sensitive and Ca^{2+} insensitive dyes (OGB-1 and SR-101, respectively). Scale bar: 10 µm, depth: ~ -250 µm. **J**, Example of spontaneous somatic Ca^{2+} activity showing the occurrence of Ca^{2+} surges (red highlight). **K**, The infusion of the vehicle did not change the frequency of astrocytes Ca^{2+} transients ($P > 0.05$ vs. pre-vehicle period, n = 5 mice) whereas ODN significantly increased their frequency ($P < 0.05$ vs. pre-ODN period, n = 6 mice). Data are represented as box-and-whisker plot (box = first and third quartiles; whisker = range). Mean values were compared using paired, two-tailed t-test.

Figure 2. ODN exacerbates ischemic damages. A, Average infarction volume when treatments are provided during the acute phase of focal cerebral ischemia, by i.c.v injection. ODN significantly increased the volume of the lesion ($P < 0.05$ vs. vehicle group; n = 8 animals/group). This effect was reversed by the selective $GABA_AR$ benzodiazepine-site antagonist flumazenil (FLZ, $P > 0.05$ vs. vehicle group, n = 10 animals). Right, representative histological analysis showing the infarction, unstained by thionine. **B**, Knockout mice for DBI ($DBI^{-}/^{-}$, the peptide precursor of ODN) were less vulnerable than wild-type mice to brain focal ischemia ($P < 0.05$ vs. WT; n = 6 animals/group), representative lesions are shown on the right. **C-F**, The

exacerbation of the damage could not be attributed to a difference in the severity of cerebral blood flow (CBF) decrease between groups during the procedure (**C**, $P > 0.05$ vs. vehicle, n = 8 animals/group). I.c.v administration of ODN produced no effect on systemic physiological parameters (**D**) such as mean arterial pressure (MAP, $P > 0.05$) or heart rate (beat *per* min., BPM, $P > 0.05$ vs. vehicle, vehicle n = 3; ODN n = 4), body temperature (**E**, $P > 0.05$ vs. vehicle, n = 8/group) or post-stroke weight loss (**F,** $P > 0.05$ vs. vehicle, n = 8/group). Data are represented as mean ± SEM. Mean values were compared using unpaired, two-tailed Mann-Whitney test (**A, B, E, F**) followed by Bonferroni's post hoc testing for multiple comparaison (**A**), or one-way ANOVA (**C, D**).

Figure 3. ODN enhances excitotoxicity and spreading depolarization waves. A, NMDA-induced striatal damages were exacerbated by co-administration of the gliopeptide ODN ($P < 0.05$; NMDA: n = 14 and NMDA+ODN: n = 13). **B**, Representative lesions are shown on the right. **C**, Intracortical infusion of KCl induced recurrent spreading depression (SD) waves: representative LFP traces showing the typical negative shift of SDs, whose number was increased in presence of ODN ($P < 0.05$, vehicle n = 6; ODN n = 6) while their amplitude remained unchanged (**D**, **E,** $P > 0.05$). Data are represented as mean ± SEM. Mean values were compared using two-tailed Mann-Whitney test.

Figure 4. Delayed and chronic treatment with ODN promotes functional recovery after stroke in young adult male mice. A, Time-line diagram of the protocol. Treatment started 3 days after the middle cerebral artery occlusion (MCAO) procedure (MCAO ODN, n = 7; MCAO vehicle n = 6) or the surgery procedure without the MCAO (sham ODN, n = 6 and sham vehicle, n = 6). ODN or its vehicle

were i.c.v injected everyday during the next 25 days (dark blue arrows). Behavioral tests were carried out at the end of each week (light blue arrows). MCAO was similar in ODN treated group and vehicle treated group (**B**). Mice treated with ODN progressively improved their performances in the execution of (**C**) the turning movement at the top of the vertical pole ($P < 0.05$ at week 4 relative to vehicle treated animals), (**D**) the descent of the vertical pole ($P < 0.05$ at week 4 relative to vehicle treated animals) and (**E**) the crossing of the horizontal beam ($P < 0.05$ at week 3 and $P < 0.01$ at week 4 relative to vehicle treated animals). Sham animals were not sensitive to ODN at any time point, and neither the surgical procedure nor the time affected their performance. Weight loss (**F,** left **,** $P > 0.05$ vs. MCAO+vehicle or Sham+vehicle; MCAO+vehicle n = 6; MCAO+ODN, n = 7; Sham+vehicle n = 6; Sham+ODN, n = 6) and mortality (**F** right, Logrank Mantel-cox test $P > 0.05$ vs. MCAO+vehicle, n = 6; MCAO+ODN, n = 7) were not different between groups at any time point. At the end of the procedure, histological analysis of mice brain showed no difference between groups for the size of the residual lesion (**G,** $P > 0.05$ vs. MCAO+vehicle; MCAO+vehicle n = 6; MCAO+ODN, n = 7), the total volume of cavities (**H**) and the atrophy of the ipsilateral hemisphere (**I**, $P > 0.05$ vs. MCAO+vehicle; MCAO+vehicle n = 6; MCAO+ODN, n = 7). Data are represented as mean ± SEM. Data were compared using Mann-Whitney test (**G**, **H**, and **I**) or nonparametric 2-way ANOVA followed by Bonferroni's post hoc testing (**B**, **F** left, **C**, **D**, **E**).

Figure 5. Delayed, chronic treatment with ODN-impregnated hydrogel promotes functional recovery after stroke in aged female mice. A. Schematic illustration of the injectable ODN-impregnated hydrogel. Infarct volume was assessed at 2 (**B**) and 6 (**C**) weeks post-stroke using cresyl violet staining. Assessment of 1 μg ODN-treated

animals showed no differences in infarct volume compared to vehicle treated controls. However, 5 μg ODN-treated animals exhibited a progressive decrease in stroke volumes with infarct volume being significantly different to vehicle-treated stroke controls 6 weeks post-stroke ($^{+}$ $P < 0.05$; n = 5 animals/group). Motor behavioral function was assessed using both the gridwalking (**D**) and cylinder tasks (**E**). On both tasks, ODN (both 1 and 5 μg) resulted in a decrease in the number of footfaults on the gridwalking task and an improvement in forelimb asymmetry in the cylinder task. As ODN is a gliopeptide with astrocyte protective features, we examine whether ODN treatment affected the extent of peri-infarct glial scaring as assessed by GFAP staining (**F-H**). Representative GFAP strained sections are shown for stroke + vehicle (**F, left**), stroke + 1 μg ODN (**F, middle**) and stroke + 5 μg ODN (**F, right**) treated animals, 2 weeks post-stroke (scale bar is 200 μm). GFAP staining intensity was assessed from layers 2/3 and 5, 0-200 μm and 800-1000 μm (each box represents 200 x 200 μm) from the stroke border at 2 (**G**) and 6 weeks (**H**) post-stroke. Treatment with ODN resulted in a dose-dependent decrease in reactive astrogliosis as assessed by GFAP-labeling 2 weeks post-stroke (**G**). No differences in GFAP-lebelling were observed at 6 weeks post-stroke between treatment groups (**H**). $^{+++}$ $P < 0.001$, compared to pre-stroke baseline behavioural controls; $^{+}$ $P < 0.05$, $^{++}$ $P < 0.01$, $^{+++}$ $P < 0.001$, compared to stroke + vehicle controls.

Figure 6. ODN dampens the stroke-induced elevation in tonic $GABA_AR$ currents in layer 2/3 pyramidal neurons. Whole-cell patch-clamp recordings were made from post-stroke brain slices, within 500 μm of infarct, from layer-2/3 pyramidal neurons. Representative traces showing the tonic inhibitory currents in control (n = 7), stroke (n = 6) and stroke + ODN (n = 6) treated animals (**A**). Tonic currents were revealed by the shift in holding currents after blocking all $GABA_ARs$ with gabazine

(SR95531; 100 μM). Box-plot (whiskers: minimum and maximum; lines: median) showing an increase in tonic inhibitory currents in peri-infarct cortical neurons that is partially dampened following exposure to ODN (**B**). Horizontal bar indicates the application of the $GABA_AR$ antagonist, SR95531. Cells were voltage-clamped at +10mV. * $P < 0.05$, *** $P < 0.001$, compared to tonic currents from control animal; + $P < 0.05$, compared to tonic currents from stroke animal.

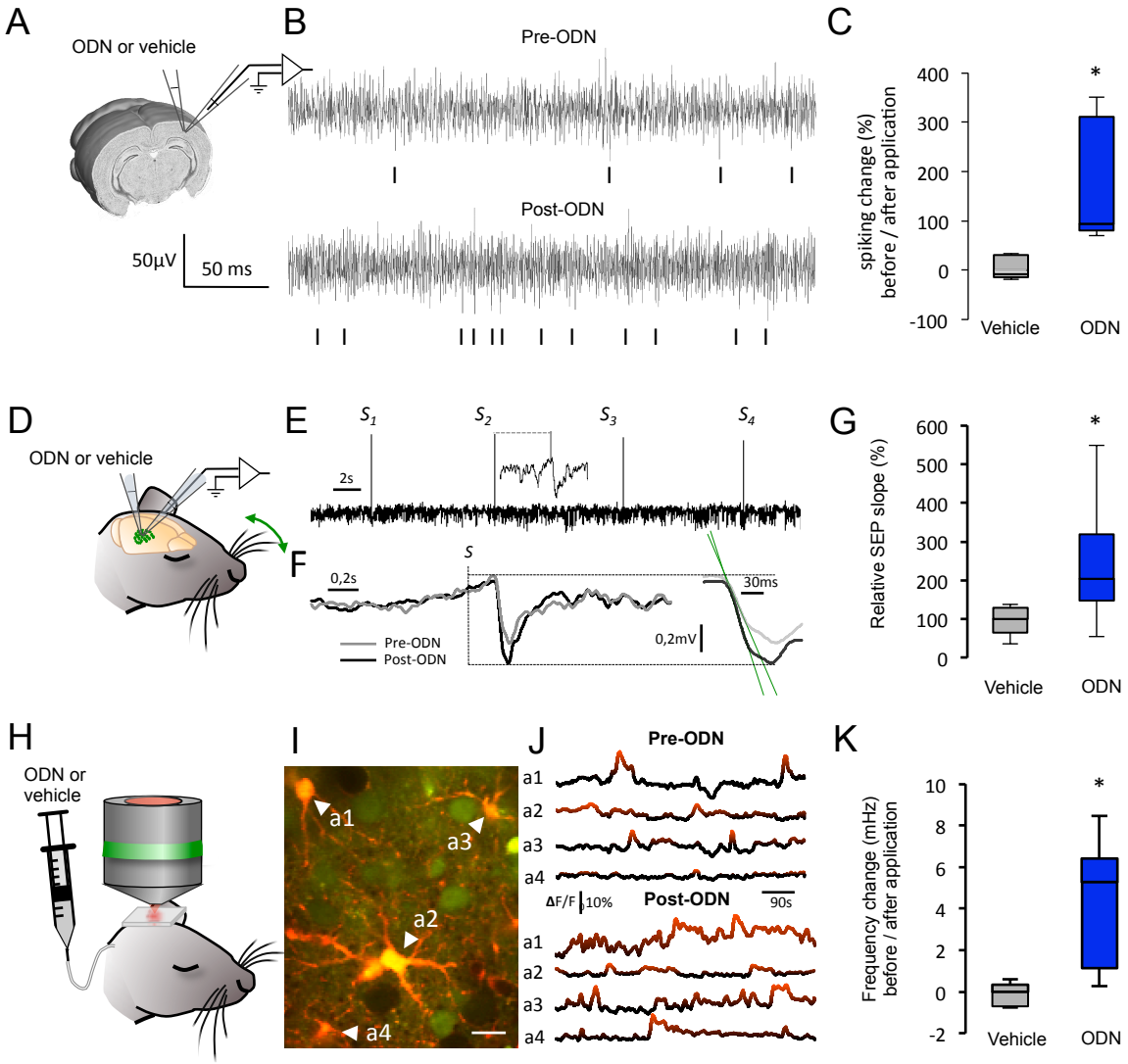

Lamtahri et al. Figure 1

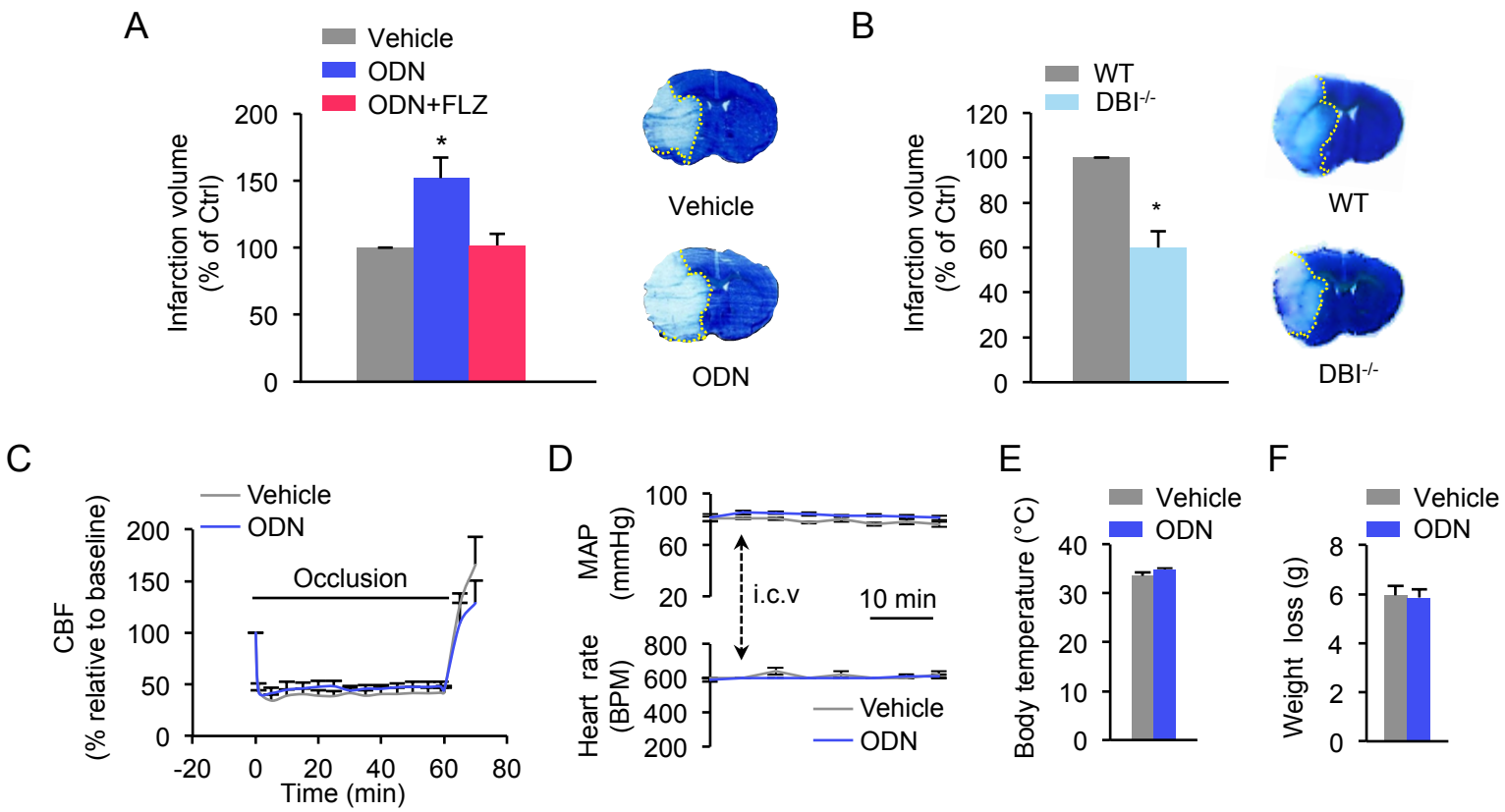

Lamtahri et al. Figure 2

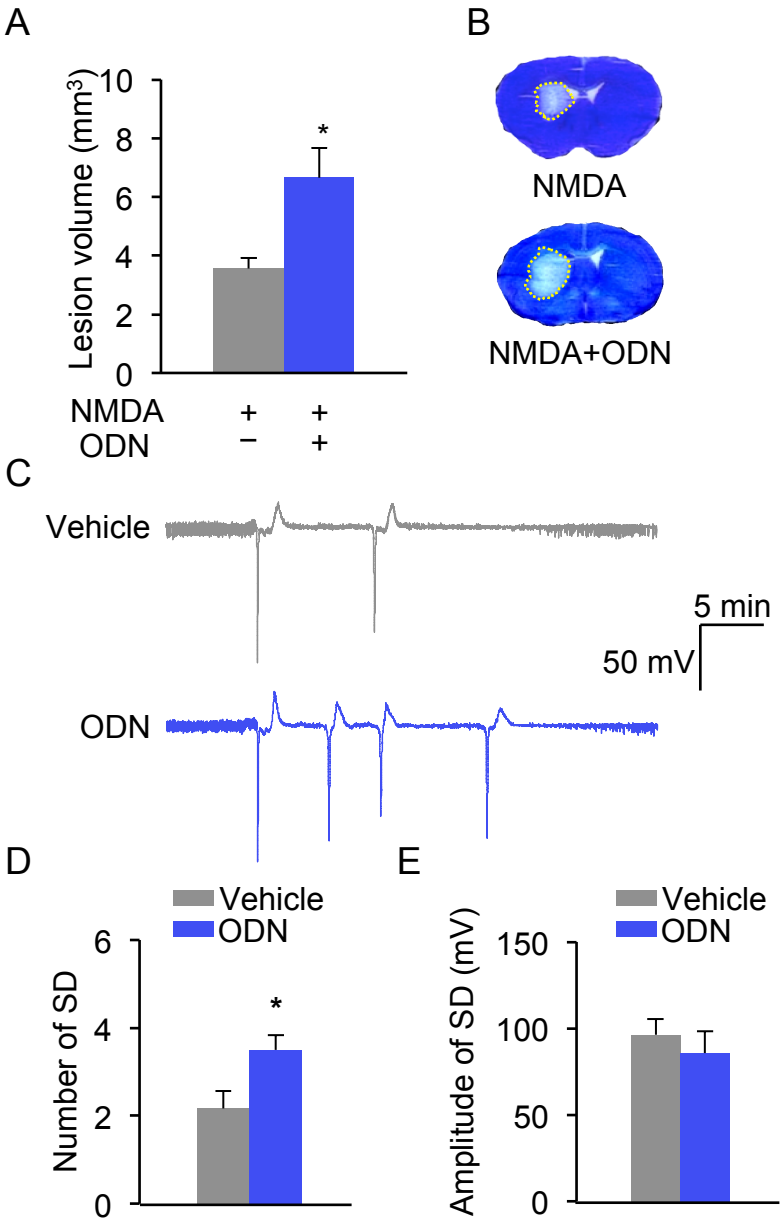

Lamtahri et al. Figure 3

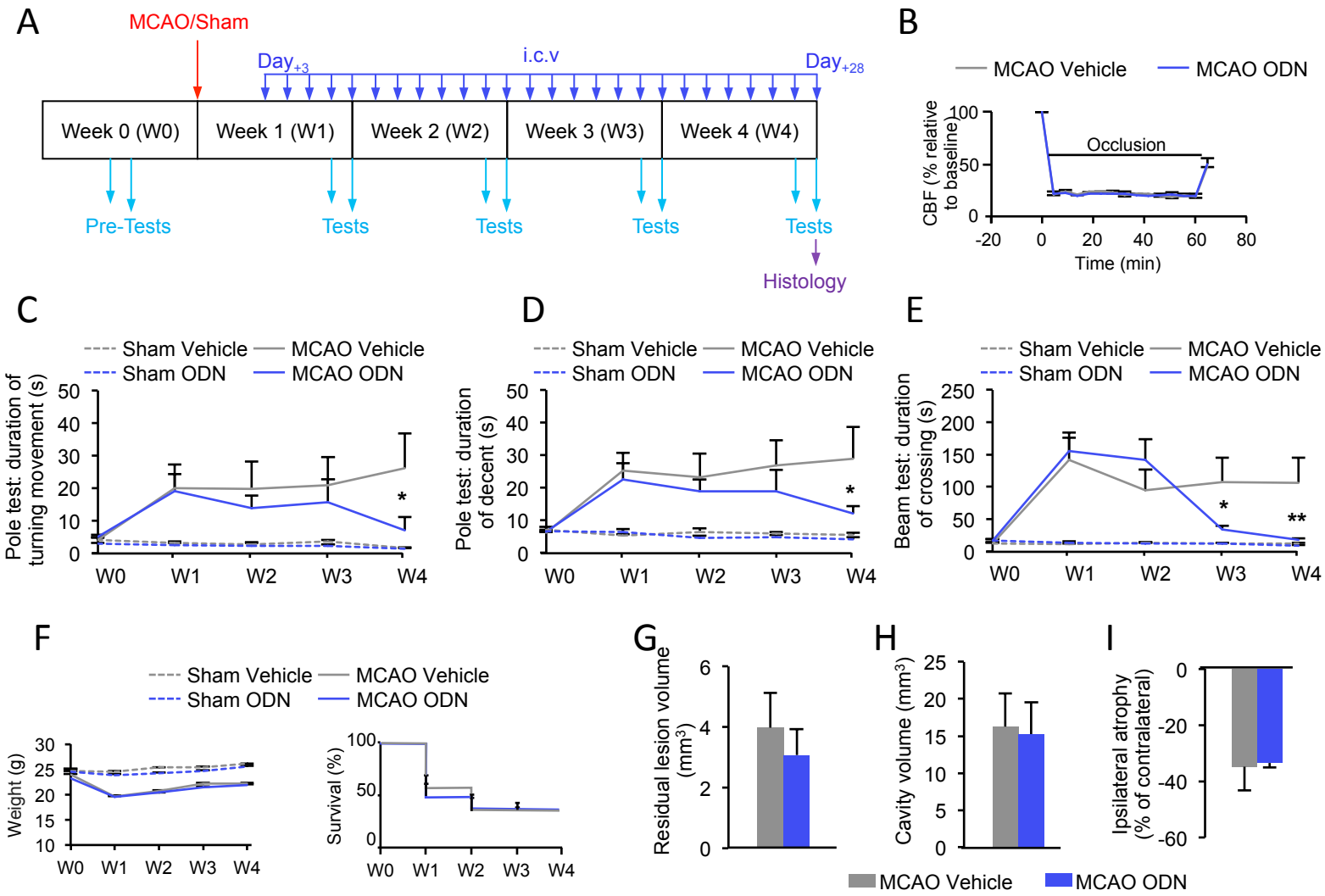

Lamtahri et al. Figure 4

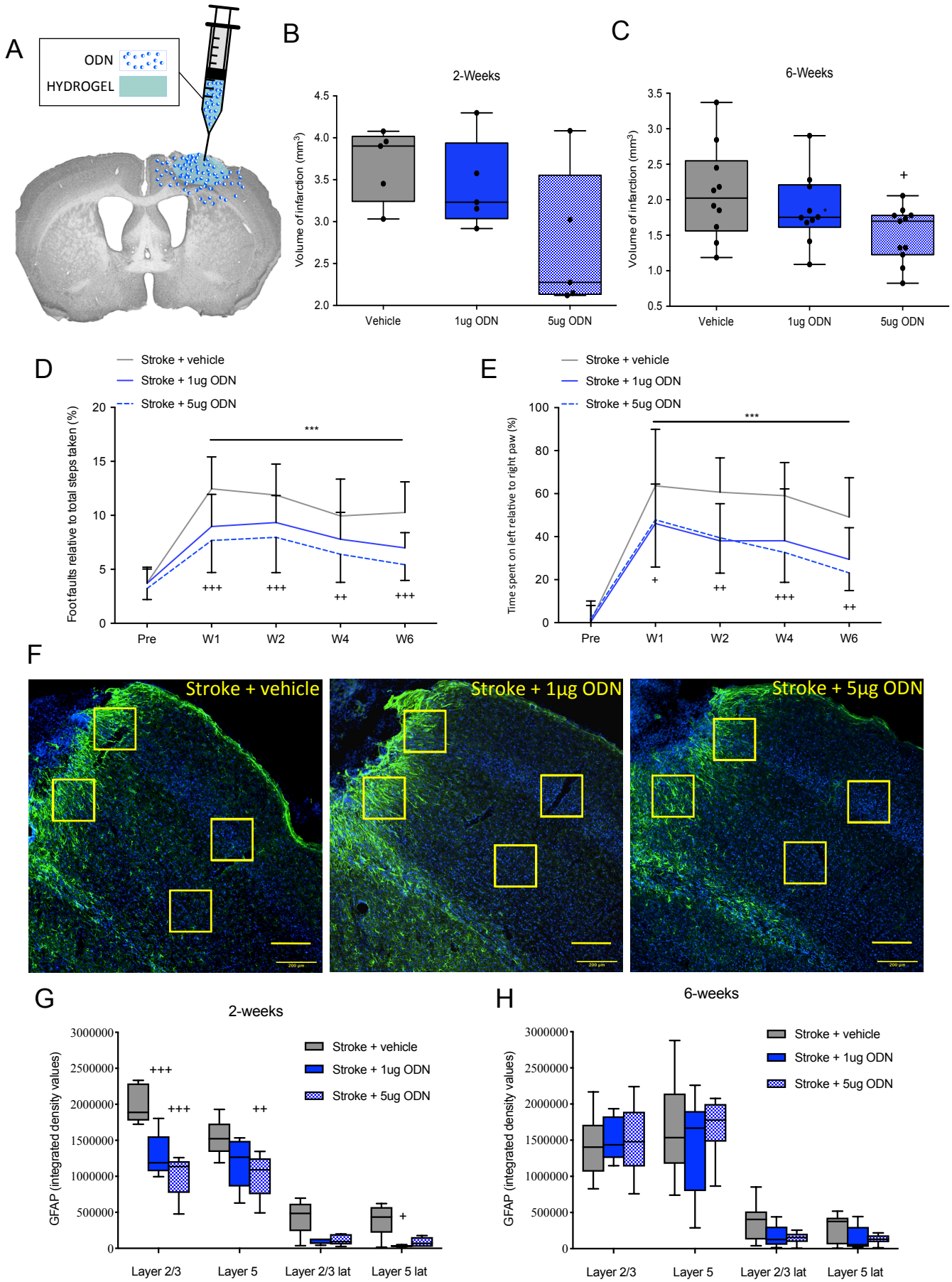

Lamtahri et al. Figure 5

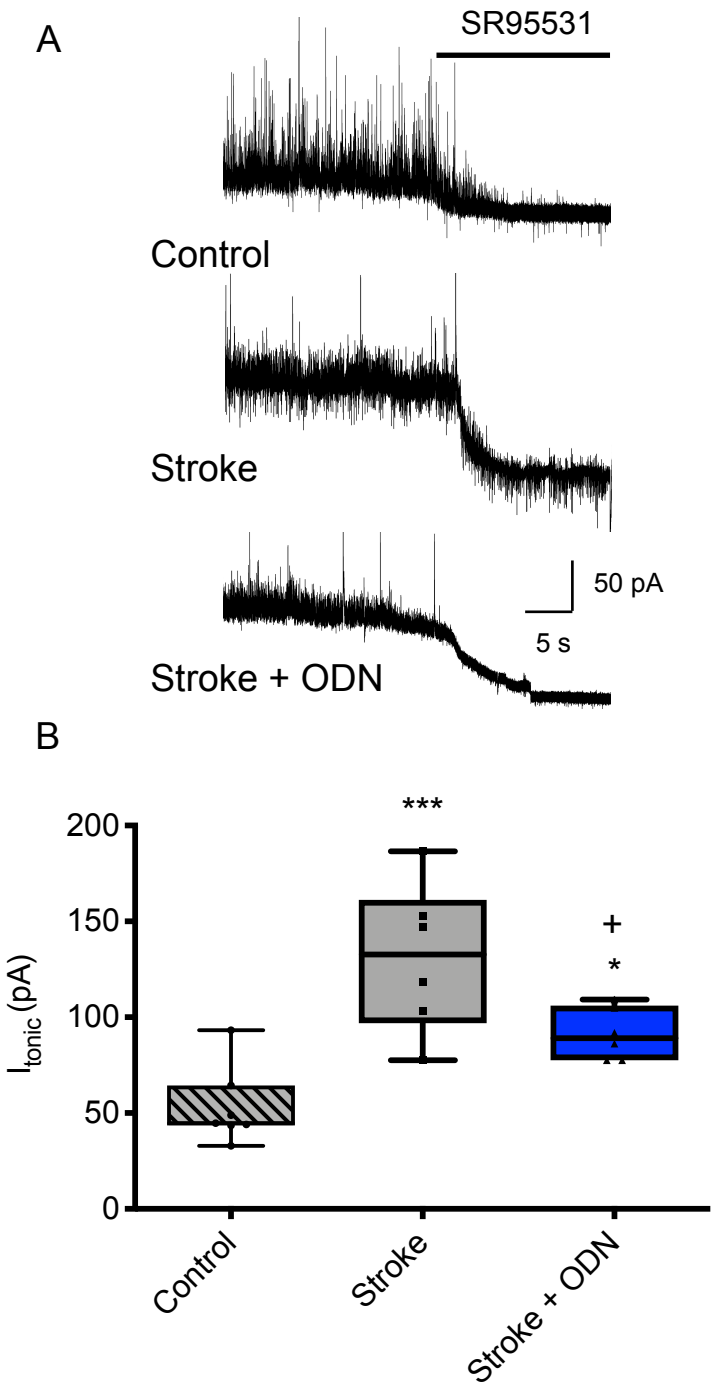

Lamtahri et al. Figure 6